J Physiol 590.7 (2012) pp 1615–1624

The Journal of Physiology

Postsynaptic mechanisms of CO_2 responses in parafacial respiratory neurons of newborn rats

Hiroshi Onimaru[1], Keiko Ikeda[2] and Kiyoshi Kawakami[3]

[1]*Department of Physiology, Showa University School of Medicine, 1-5-8 Hatanodai, Shinagawa-ku, Tokyo 142, Japan*
[2]*Division of Biology, Hyogo College of Medicine, 1-1 Mukogawa-cho, Nishinomiya, Hyogo 663-8501, Japan*
[3]*Division of Biology, Centre for Molecular Medicine, Jichi Medical University, Shimotsuke, Tochigi 329-0498, Japan*

Key points

- The central chemoreceptors for respiratory control in the medulla sense changes in CO_2 concentration and regulate respiratory activity.
- Neurons that express a transcription factor, Phox2b, in the parafacial region of the rostral and ventrolateral medulla are excited by hypercapnic stimulation and are proposed to play an important role in central chemoreception.
- In this study, we show evidence that Phox2b-expressing parafacial neurons in neonatal rats were sensitive to hypercapnia via direct action on the postsynaptic membrane without contribution of putative presynaptic or other calcium-dependent components.
- Since these parafacial neurons are also a part of the respiratory rhythm generator in neonates, they are essential for postnatal survival, which is probably due to their contribution to central chemoreception as well as respiratory rhythm generation.

Abstract The parafacial respiratory group (pFRG) in the rostral ventrolateral medulla of the newborn rat is predominantly composed of pre-inspiratory (Pre-I) neurons and is involved in respiratory rhythm generation. The subgroup located close to the ventral surface (at least partially overlapping the retrotrapezoid nucleus, RTN) expresses the Phox2b transcription factor and responds to hypercapnic stimulation with strong depolarization, which suggests it has a role in central chemoreception. Although a CO_2 response of pFRG/RTN neurons has been confirmed in the presence of tetrodotoxin (TTX), it is unknown whether the depolarization involved in this response is induced by a direct postsynaptic response of pFRG/RTN neurons or by any presynaptic components mediated by Ca^{2+}-dependent mechanisms. In this study, we examined the effects of ATP or substance P receptor antagonists on hypercapnic responses of rostral pFRG/RTN neurons. We tested effects of Cd^{2+} and low Ca^{2+}–high Mg^{2+} in the presence of TTX. The experiments were performed in *in vitro* brainstem–spinal cord preparations from newborn rats in which Pre-I neurons reflect the discharge pattern of the pFRG. We found that ATP receptor and substance P receptor antagonists do not block membrane potential responses to hypercapnic stimulation (2% → 8%) of pFRG/RTN neurons in the rostral parafacial region. Moreover, rostral pFRG/RTN neurons were depolarized by hypercapnia under conditions where the contribution of presynaptic components was inhibited in the presence of TTX and Cd^{2+} or in a low Ca^{2+}–high Mg^{2+} solution containing TTX and Cd^{2+}. All cases (except some cases in a low Ca^{2+}–high Mg^{2+} solution) of membrane depolarization by hypercapnic stimulation were accompanied with an increase in input resistance. These neurons were predominantly Phox2b immunoreactive. Our findings

DOI: 10.1113/jphysiol.2011.222687

suggest that the response of pFRG/RTN neurons to hypercapnia is induced by direct action on the postsynaptic membrane via closing of K^+ channels.

(Received 18 October 2011; accepted after revision 3 February 2012; first published online 6 February 2012)
Corresponding author H. Onimaru: Department of Physiology, Showa University School of Medicine, 1-5-8 Hatanodai, Shinagawa-ku, Tokyo 142, Japan. Email: oni@med.showa-u.ac.jp

Abbreviations: ACSF, artificial cerebrospinal fluid; AICA, anterior inferior cerebellar artery; C4, fourth cervical ventral root; NK1, neurokinin-1; PBS, phosphate buffer solution; pFRG, parafacial respiratory group; PPADS, pyridoxalphosphate-6-azophenyl-2′,4′-disulfonic acid; Pre-I, pre-inspiratory; RTN, retrotrapezoid nucleus; TTX, tetrodotoxin.

Introduction

The parafacial respiratory group (pFRG) in the rostral ventrolateral medulla of the neonatal rat is predominantly composed of pre-inspiratory (Pre-I) neurons and is involved in respiratory rhythm generation (Onimaru & Homma, 2003). Of particular interest is the subgroup located close to the ventral surface, which at least partially overlaps the retrotrapezoid nucleus (RTN) in adult rats (Stornetta *et al.* 2006). This subgroup of the pFRG as well as adult RTN neurons (hereinafter referred to as pFRG/RTN neurons) express a transcription factor, Phox2b, and respond to high CO_2 stimulation with strong depolarization, which is suggestive of a role in central chemoreception (Mulkey *et al.* 2004; Stornetta *et al.* 2006; Onimaru *et al.* 2008, 2009). Although the CO_2 response of pFRG/RTN neurons has previously been confirmed in the presence of tetrodotoxin (TTX), it remains to be elucidated whether the depolarization was induced by a direct postsynaptic response of pFRG/RTN neurons or by any presynaptic components mediated by a Ca^{2+}-dependent mechanism. Gourine *et al.* (2010) showed that a decreased pH in the brainstem chemoreceptor area induced an increase in intracellular Ca^{2+} concentration and release of ATP. Thus, ATP is one of the important presynaptic components that affect chemosensitivity of neurons in the ventral medulla (Guyenet *et al.* 2010*a*). It was reported that the response of Phox2b-positive neurons in the RTN induced by lowering the pH was inhibited by application of ATP receptor blockers (Gourine *et al.* 2010). Alternatively, Mulkey *et al.* (2004) reported that pH sensitivity of RTN neurons was not affected by ATP receptor blockers. Another candidate presynaptic component of chemosensitivity is substance P, because neurokinin-1 (NK1) receptor-expressing neurons in the ventral medulla are essential for normal central chemoreception in the conscious rat (Nattie & Li, 2006). Phox2b-positive cells in the RTN express NK1 receptors (Onimaru *et al.* 2008; Takakura *et al.* 2008), and substance P was still able to activate the chemosensitive RTN neurons in the presence of blockers of excitatory and inhibitory transmitters (Mulkey *et al.* 2007). Moreover, substance P can induce a depolarizing response in the pFRG/RTN neurons similar to the response to hypercapnic stimulation (Onimaru *et al.* 2009). Thus, hypercapnic stimulation may cause the effect by releasing substance P from presynaptic sites by a calcium-dependent mechanism. Therefore, in the present study, we examined the effects of ATP receptor antagonists (MRS2179 and pyridoxalphosphate-6-azophenyl-2′,4′-disulfonic acid (PPADS) (Gourine *et al.* 2010), and substance P antagonists (L-703606 and spantide) on the CO_2/H^+ response. Furthermore, we tested the effects of Cd^{2+} and low Ca^{2+}–high Mg^{2+} in the presence of TTX.

Methods

Experimental protocols were approved by the Animal Research Committee of Showa University, which operates in accordance with Law No. 105 of the Japanese Government for the care and use of laboratory animals and conformed to the principles of UK regulations, as described in Drummond (2009). All efforts were made to minimize the number of animals used and their suffering.

Preparations

Experiments were performed with brainstem–spinal cord preparations from 0 to 4-day-old Wistar rats. Newborn rats were deeply anaesthetized with ether. The brainstem and spinal cord were isolated and superfused at a rate of 3.0 ml min^{-1} with the following artificial cerebrospinal fluid (ACSF) (in mM): 124 NaCl, 5.0 KCl, 1.2 KH_2PO_4, 2.4 $CaCl_2$, 1.3 $MgCl_2$, 26 $NaHCO_3$ and 30 glucose, equilibrated with 95% O_2 and 5% CO_2, pH 7.4, at 26–27°C. The preparations were cut transversely at a level just rostral to the anterior inferior cerebellar artery (AICA) with a custom-made vibratome (Fig. 1). This cut was equivalent to a position approximately 0.5 mm rostral to the caudal end of the facial nucleus that corresponds to the level of the Xth cranial nerve root (Ruangkittisakul *et al.* 2006; Ballanyi *et al.* 2009).

Electrophysiology

Inspiratory activity correlating with phrenic nerve activity was monitored from the fourth cervical ventral root (C4)

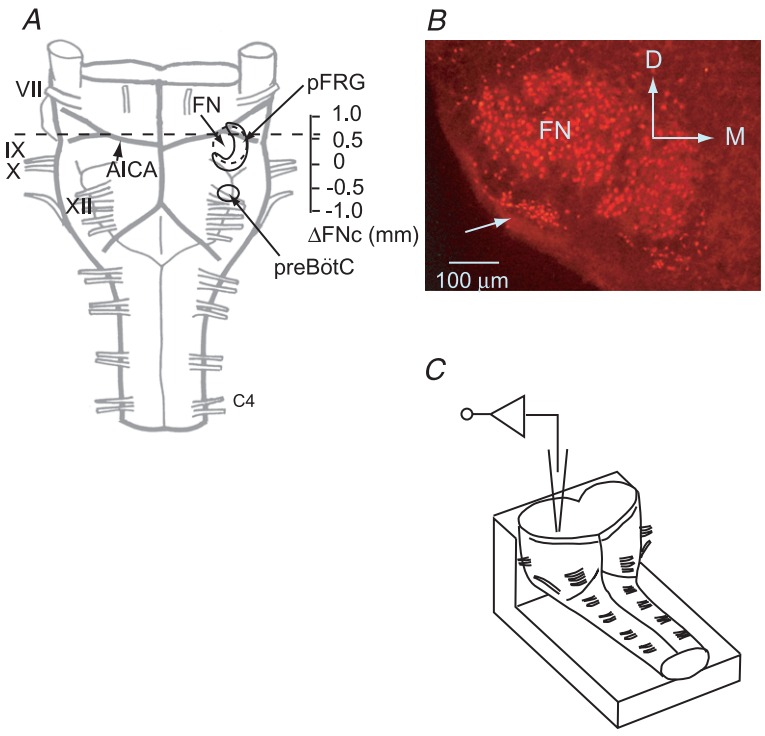

Figure 1. Preparation and positioning of a transverse section
A, ventral view of a brainstem–spinal cord preparation from a neonatal rat. The preparation was cut at the level of the dotted line. *B*, rostral cut surface view of Phox2b-immunoreactive (-ir) cells at a level 0.5 mm rostral to the caudal end of the facial nucleus (ΔFNc). Phox2b-ir cells (red) are located in the ventral parafacial region (arrow) and in the facial nucleus. *C*, schematic representation of the preparation in the recording chamber. The preparation was fixed onto a rubber block by pins with the cut surface facing up for whole-cell recordings of the parafacial region via the cut surface of the cross section. AICA, the anterior inferior cerebellar artery; FN, facial nucleus; pFRG, parafacial respiratory group; preBötC, preBötzinger complex; VII–XII, cranial nerves; C4, the fourth cervical ventral root; D, dorsal; M, medial.

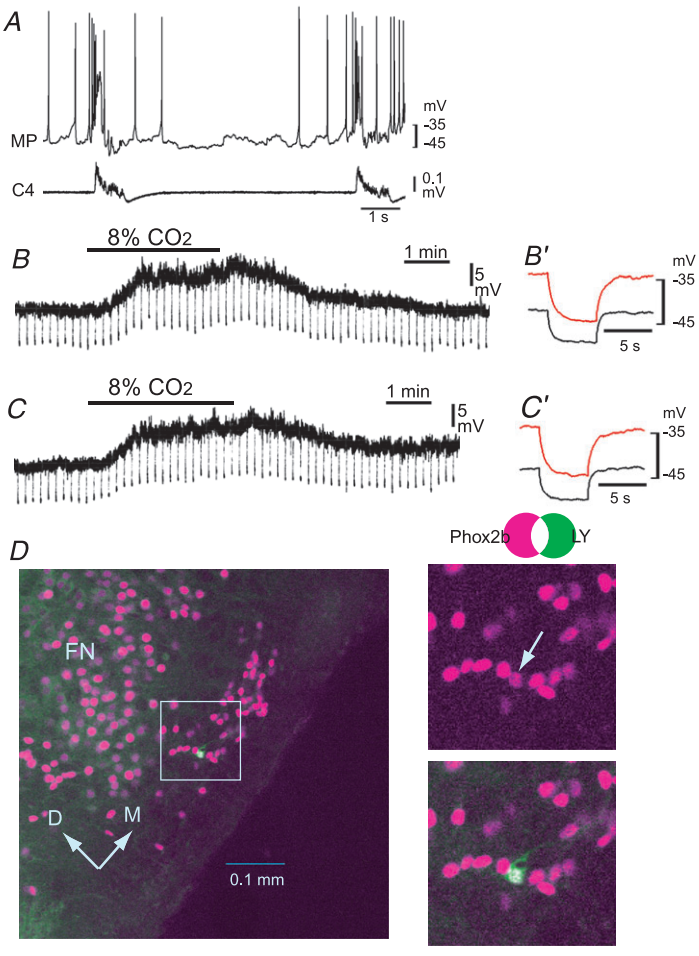

Figure 2. Effects of an ATP receptor antagonist (MRS2179) on the CO_2/H^+ response of a rostral pFRG/RTN neuron
A, burst pattern in control solution. MP, membrane potential trace; C4, fourth cervical ventral root activity. *B*, membrane potential response to hypercapnic stimulation (2% CO_2 → 8% CO_2) in the presence of 0.5 μM TTX. Negative deflections of the baseline membrane potential are proportional to input resistance. *B′*, a faster sweep representation (average of 5 traces) of the membrane potential response to application of 20 pA hyperpolarizing square current pulses in 2% CO_2 (black trace) and 8% CO_2 (red trace). Note that application of 8% CO_2 induced membrane depolarization and an increase in input resistance. *C*, membrane potential responses to hypercapnic stimulation in the presence of TTX plus 20 μM MRS2179. *C′*, a faster sweep representation (average of 5 traces) of the membrane potential response to application of 20 pA hyperpolarizing square current pulses in 2% CO_2 (black trace) and 8% CO_2 (red trace). Note that the depolarizing response to 8% CO_2 was preserved. *D*, location of the recorded neuron stained by Lucifer yellow (LY, green). This neuron is Phox2b positive (magenta). Right panels, higher magnification of the highlighted square in the left image. FN, facial nucleus; D, dorsal; M, medial.

Table 1. Effects of receptor antagonists on hypercapnic responses of rostral pFRG/RTN neurons

	Control		20 μM MRS2179 ($n = 5$)	
	2%	8%	2%	8%
V_m (mV)	−43.2 ± 1.3	−33.6 ± 3.6**	−41.6 ± 1.1	−33.0 ± 4.5*
R_m (MΩ)	324 ± 48.7	444 ± 84.7*	350 ± 70.7	490 ± 124*
	Control		0.1 mM PPADS ($n = 5$)	
	2%	8%	2%	8%
V_m (mV)	−48.6 ± 3.9	−38.4 ± 4.2**	−48.2 ± 3.8	−37.8 ± 5.9*
R_m (MΩ)	466 ± 321	719 ± 399*	458 ± 252	642 ± 328*
	Control		0.4 μM spantide ($n = 4$)	
	2%	8%	2%	8%
V_m (mV)	−46.3 ± 3.0	−32.8 ± 7.2*	−45.0 ± 3.9	−32.0 ± 5.7*
R_m (MΩ)	412 ± 131	775 ± 126*	295 ± 90.0	505 ± 204*
	Control		2 μM L-703606 ($n = 4$)	
	2%	8%	2%	8%
V_m (mV)	−45.3 ± 2.1	−37.7 ± 1.2*	−44.0 ± 2.0	−37.0 ± 4.4*
R_m (MΩ)	450 ± 150	650 ± 132	467 ± 153	617 ± 275

*$P < 0.05$; **$P < 0.01$.

(Suzue, 1984). Membrane potentials and input resistances of neurons in the parafacial region of the rostral medulla were recorded by a blind whole-cell patch-clamp method (Onimaru & Homma, 1992) (Fig. 1). Respiratory-related bursting neurons in the rostral pFRG were approached from the rostral cut surface by monitoring extracellular action potential discharges. Most of the bursting neurons in this region were characterized by pre- and post-inspiratory discharges of variable length, and thus they were considered to be in the same category as Pre-I neurons in previous reports (e.g. Onimaru & Homma, 1992). They received heterogeneous synaptic inputs during the inspiratory phase and more than 70% of them in this region showed only weak inspiratory inhibition (Onimaru *et al.* 2008; Onimaru & Dutschmann, 2012). The electrodes (inner tip diameter, 1.2–2.0 μm; resistance, 4–8 MΩ) were filled with the following pipette solution (in mM): 130 potassium gluconate, 10 EGTA, 10 Hepes, 2 Na_2-ATP, 1 $CaCl_2$ and 1 $MgCl_2$, with pH 7.2–7.3 adjusted with KOH. Membrane potentials were recorded with a single-electrode voltage-clamp amplifier (CEZ-3100; Nihon Kohden Corp., Tokyo, Japan) after compensation for series resistance (20–50 MΩ) and capacitance. After establishment of the whole-cell recordings, the standard solution (5% CO_2, pH 7.4) was replaced by an ACSF containing 0.5 μM TTX equilibrated with 2% CO_2 (pH 7.8). Effects of antagonists were examined by the two following steps. (1) Control hypercapnic stimulation: After a 15 min incubation with the 2% CO_2 solution, the superfusate was replaced by a hypercapnic acidic ACSF equilibrated with 8% CO_2 (pH 7.2). After a 5–6 min test of membrane potential responses in the 8% CO_2 solution, the superfusate was returned to a 2% CO_2 solution (Onimaru *et al.* 2008). (2) Effects of antagonists: The same procedure as the above control CO_2 test was performed in the presence of antagonists, i.e. 15 min pre-treatment in 2% CO_2 + antagonists. To examine effects of blockade of Ca^{2+} channel activation on hypercapnic responses, 0.5 mM Cd^{2+} or 0.5 mM Cd^{2+} plus low Ca^{2+} (0.2 mM) and high Mg^{2+} (5 mM) in the presence of 0.5 μM TTX (2% CO_2) were superfused for more than 15 min before hypercapnic stimulation (8% CO_2). This test was performed without the control CO_2 test in normal ACSF, because we found it was difficult to maintain whole-cell recordings for long periods in these conditions due to unknown reasons. In all experiments using TTX, a square current pulse (500 ms, 0.1 Hz, 20–40 pA) was applied to monitor changes in input resistance. Values are presented as mean ± SD. Significance values ($P < 0.05$) were determined with a Student's *t* test.

For histological analysis of the recorded cells, the electrode tips were filled with 0.2% Lucifer yellow (lithium salt, Sigma-Aldrich, Japan). After the experiments, preparations were fixed for 2–3 h at 4°C in 4% paraformaldehyde in 0.1 M phosphate buffer solution (PBS), transferred into 18% sucrose–PBS (overnight) and

cut into 50-μm-thick transverse sections for immunofluorescent detection.

Immunofluorescence

The primary antibodies used for immunofluorescence were rabbit anti-Lucifer yellow (1:400 dilution, Molecular Probes/Invitrogen, Carlsbad, CA, USA) and guinea pig anti-Phox2b (1:1000 dilution) as described previously (Onimaru *et al.* 2008). The secondary antibodies for fluorescence staining (1:1000 dilutions) were Alexa Fluor 488 anti-rabbit IgG or Alexa Fluor 546 anti-rabbit IgG, and Alexa Fluor 633 anti-guinea pig IgG or Alexa Fluor 546 anti-guinea pig IgG (Molecular Probes/Invitrogen). Images of the immunofluorescent samples were obtained with 10× or 20× objectives on an Olympus FV1000 confocal microscope (Olympus Optical, Tokyo, Japan) or Olympus BX60 conventional fluorescence microscope (Olympus Optical).

Results

Effects of ATP receptor antagonists on the CO_2 response of rostral pFRG/RTN neurons

We examined two kinds of ATP receptor antagonists (MRS2179 and PPADS) on the CO_2 response of rostral pFRG/RTN neurons. In response to hypercapnia (2% → 8% CO_2), the rostral pFRG/RTN neurons ($n = 5$) were depolarized by 10.2 ± 4.9 mV in control solution (0.5 μM TTX) and by 10.4 ± 5.5 mV in TTX plus an ATP receptor antagonist, 20 μM MRS2179 (Fig. 2). The input resistance during hypercapnia increased to 154% in control TTX solution and 140% in TTX plus MRS2179 (Table 1). In another set of experiments, similarly, hypercapnic stimulation depolarized the rostral pFRG/RTN neurons ($n = 5$) by 9.5 ± 4.4 mV in 0.5 μM TTX (control) and by 8.6 ± 5.2 mV in TTX plus an ATP receptor antagonist, 0.1 mM PPADS, (Fig. 3). The input resistance increased to 137% in control and 140% with PPADS (Table 1). Thus, the CO_2 responses of rostral pFRG/RTN neurons were

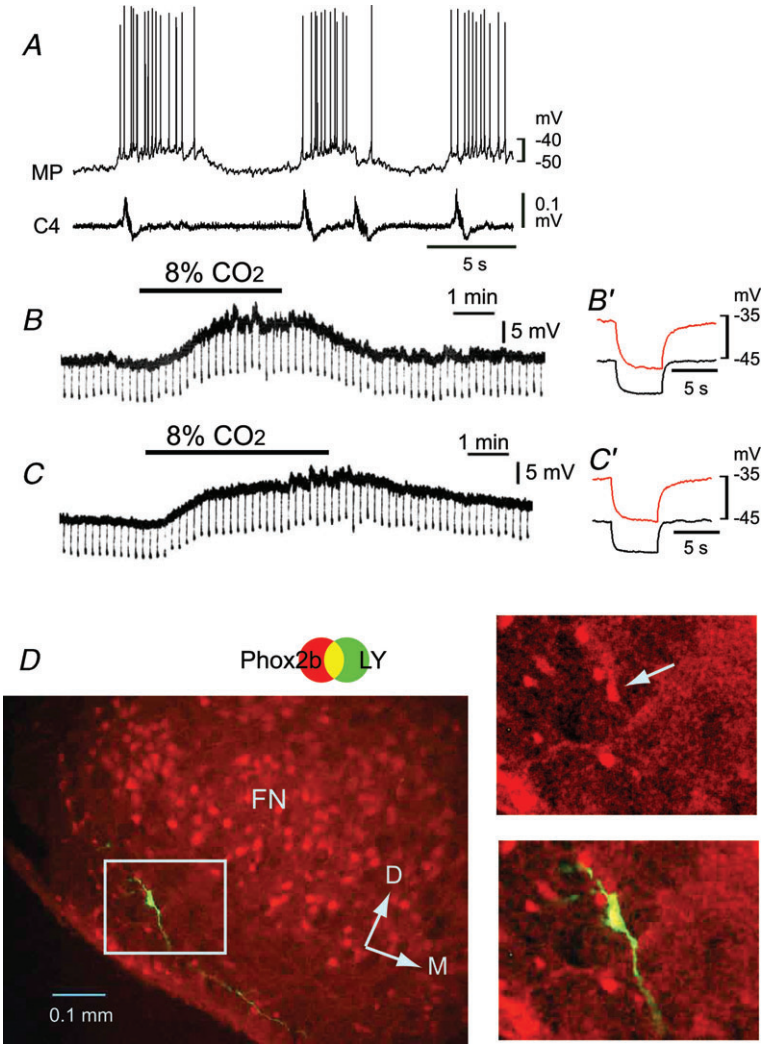

Figure 3. Effects of an ATP receptor antagonist (PPADS) on the CO_2/H^+ response of a rostral pFRG/RTN neuron
A, burst pattern in control solution. MP, membrane potential trace; C4, fourth cervical ventral root activity. *B*, membrane potential response to hypercapnic stimulation (2% CO_2 → 8% CO_2) in the presence of 0.5 μM TTX. Negative deflections of the baseline membrane potential are proportional to input resistance. *B′*, a faster sweep representation (average of 5 traces) of the membrane potential response to application of 20 pA hyperpolarizing square current pulses in 2% CO_2 (black trace) and 8% CO_2 (red trace). Note that application of 8% CO_2 induced membrane depolarization and an increase in input resistance. *C*, membrane potential responses to hypercapnic stimulation in the presence of TTX plus 0.1 mM PPADS. *C′*, faster sweep representation (average of 5 traces) of the membrane potential response to application of 20 pA hyperpolarizing square current pulses in 2% CO_2 (black trace) and 8% CO_2 (red trace). Note that the depolarizing response to 8% CO_2 was preserved. *D*, location of the recorded neuron stained by Lucifer yellow (LY, green). This neuron is Phox2b positive (red). Right panels, higher magnification of the highlighted square in the left image. FN, facial nucleus; D, dorsal; M, medial.

preserved in the presence of ATP receptor antagonists (MRS2179 or PPADS). Eight neurons out of the ten examined were successfully stained by Lucifer yellow and were confirmed to be Phox2b immunoreactive.

Effects of NK1 receptor antagonists on the CO_2 response of rostral pFRG/RTN neurons

Substance P (50 nM), in the presence of TTX, induced membrane depolarization of rostral pFRG/RTN neurons (15 ± 1.2 mV, $n = 4$, Fig. 4*C*), which was accompanied by an increase in the input resistance to 153%. We examined effects of substance P antagonists on the hypercapnic response of pFRG/RTN neurons. The depolarizing response to hypercapnic stimulation (2% → 8% CO_2) of the rostral pFRG/RTN neurons (13.5 ± 7.3 mV with 188% increase in input resistance, $n = 4$, in TTX) was preserved (13.0 ± 4.9 mV with 167% increase in input resistance) after the effect of substance P was inhibited by treatment with 0.4 μM spantide in TTX (Fig. 4*D*, Table 1). Similarly, the hypercapnic response of the rostral pFRG/RTN neurons was also preserved after treatment with 2 μM L-703606 (depolarization of 7.7 ± 2.1 mV; input resistance increase to 144%; $n = 3$) (Table 1). Six out of seven neurons were stained successfully by Lucifer yellow and confirmed as Phox2b immunoreactive, whereas one neuron was not Phox2b immunoreactive.

CO_2 response of rostral pFRG/RTN neurons in the presence of TTX and Cd^{2+}

In the presence of 0.5 μM TTX and 0.1 mM Cd^{2+}, hypercapnic stimulation (2% → 8% CO_2) depolarized the rostral pFRG/RTN neurons ($n = 9$) by 8.8 ± 2.7 mV with a 146% increase in the input resistance (377 ± 115 MΩ in 2% CO_2 and 551 ± 186 MΩ in 8% CO_2, $P < 0.01$) (Fig. 5). All but one of these neurons were Phox2b immunoreactive. Furthermore, we examined the CO_2 response of

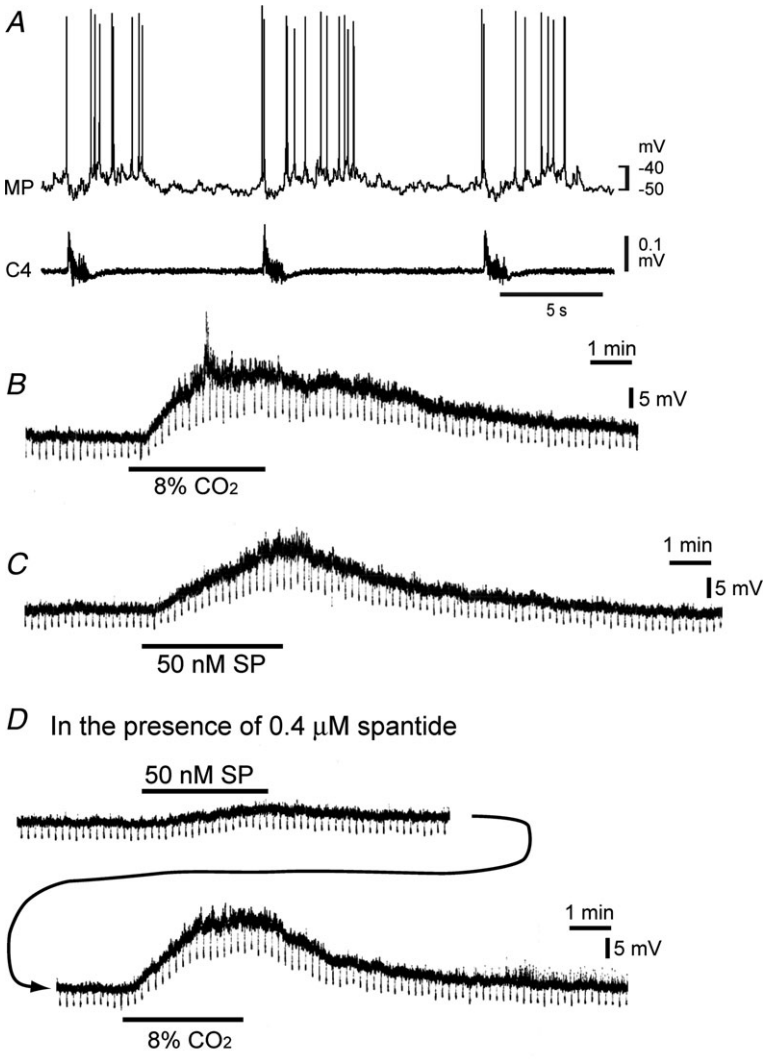

Figure 4. Effects of the substance P receptor antagonist (spantide) on the CO_2/H^+ response of a rostral pFRG/RTN neuron
A, burst pattern in control solution. MP, membrane potential trace; C4, fourth cervical ventral root activity. *B*, membrane potential response to hypercapnic stimulation (2% CO_2 → 8% CO_2) in the presence of 0.5 μM TTX. Negative deflections of the baseline membrane potential are proportional to input resistance. Note that application of 8% CO_2 induced membrane depolarization and an increase in input resistance. *C*, membrane potential responses to bath application of 50 nM substance P (SP) in the presence of TTX. Note that the membrane potential response is similar to hypercapnia. *D*, in the presence of 0.4 μM spantide (20 min), membrane depolarization by 50 nM substance P was significantly reduced, but hypercapnia (2% CO_2 → 8% CO_2) still induced membrane depolarization.

eight rostral pFRG/RTN neurons after treatment with low Ca^{2+} and high Mg^{2+} in the presence of TTX and Cd^{2+} (Fig. 6). These neurons were depolarized by 7.8 ± 3.7 mV in response to hypercapnic stimulation (2% → 8% CO_2). The input resistance was increased in four neurons (to 127% of control) but not in another four neurons (93% of control) (Fig. 7). The average change in the input resistance in eight neurons was not significant (356 ± 105 MΩ in 2% CO_2 *versus* 389 ± 146 MΩ in 8% CO_2). These neurons were confirmed to be Phox2b immunoreactive.

Discussion

ATP receptor and substance P receptor antagonists could not block the CO_2 response of bursting neurons in the rostral pFRG/RTN. Moreover, rostral pFRG/RTN neurons were depolarized by hypercapnia under conditions whereby the contribution of presynaptic components were inhibited in the presence of TTX and Cd^{2+} or in low Ca^{2+}–high Mg^{2+} solution containing TTX and Cd^{2+}. Most of these neurons were Phox2b immunoreactive. The main limitations of the present study were: (1) the use of neonates (P0–P4) in *in vitro* preparations in which glial components in the central chemoreceptor region of the medulla may be immature in comparison to adults; and (2) the fact that the temperature of the superfusate was low (26°C) (Guyenet *et al.* 2010*b*).

A recent study by Gourine *et al.* (2010) showed strong evidence that ATP released from astrocytes in the chemoreceptor area of the ventral medulla acts as an essential factor for central chemosensory transduction. It was shown that the pH response of Phox2b-positive neurons in the RTN of organotypic cultured slices from rat pups (8–10 days old) was blocked by ATP receptor antagonists (MRS2179 and PPADS). Moreover, Wenker *et al.* (2010) suggested that astrocytes in the RTN sense CO_2/H^+ in part by inhibition of a Kir4.1–Kir5.1-like current in slice preparations from 7- to 12-day-old rats. They also found that ATP receptor antagonists (PPADS and suramin) decreased CO_2 sensitivity of RTN neurons and suggested that RTN astrocytes may provide an excitatory purinergic drive to pH-sensitive RTN neurons. In contrast, Mulkey *et al.*

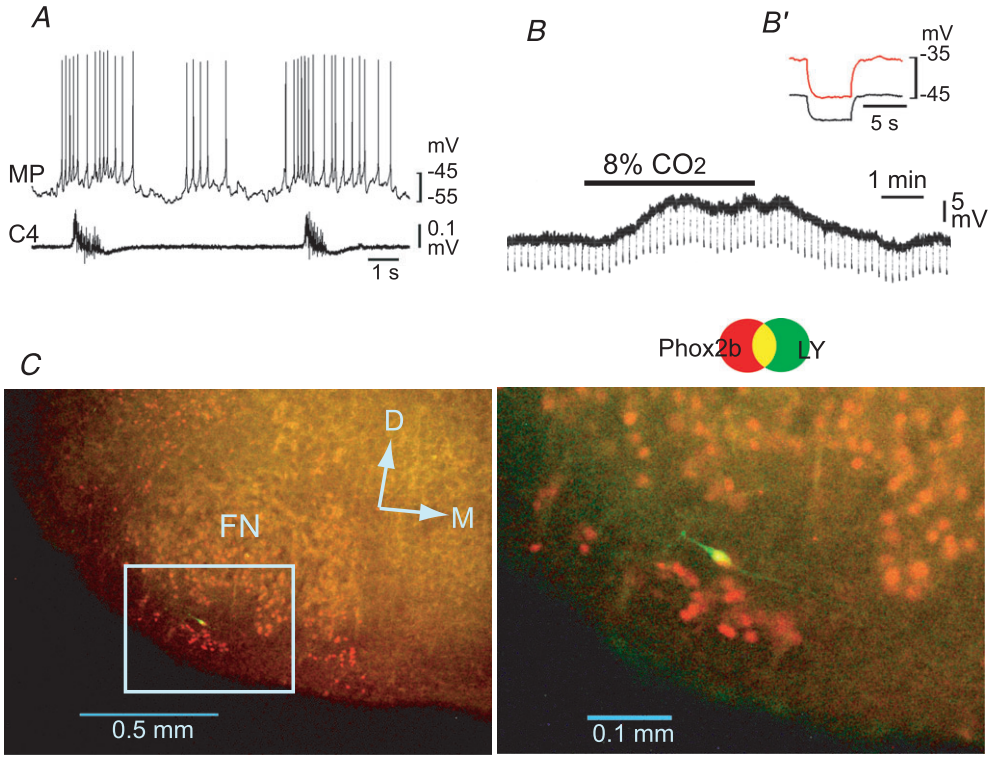

Figure 5. Effects of Cd^{2+} on the CO_2/H^+ response of a rostral pFRG/RTN neuron
A, burst pattern in control solution. MP, membrane potential trace; C4, fourth cervical ventral root activity. *B*, membrane potential response to hypercapnic stimulation (2% CO_2 → 8% CO_2) in the presence of 0.5 μM TTX + 0.1 mM Cd^{2+}. Negative deflections of the baseline membrane potential are proportional to input resistance. *B′*, a faster sweep representation (average of 5 traces) of the membrane potential response to application of 20 pA hyperpolarizing square current pulses in 2% CO_2 (black trace) and 8% CO_2 (red trace). Note that application of 8% CO_2 induced membrane depolarization and an increase in input resistance. *C*, location of a recorded neuron stained by Lucifer yellow (LY, green). This neuron is Phox2b positive (red). Right panel, higher magnification of the highlighted square in the left image. FN, facial nucleus; D, dorsal; M, medial.

(2004) previously reported that the pH sensitivity of the RTN neurons in slices from 7- to 12-day-old rats was not blocked by PPADS. Regarding this apparent discrepancy, Wenker *et al.* (2010) suggested that effects of ATP receptor antagonists in the studies above depend on the buffers used (i.e. less effective in Hepes buffer than bicarbonate buffer). Although we used bicarbonate-buffered media and preparations from 0- to 4-day-old rats, our results demonstrated that ATP receptor antagonists could not block membrane depolarization of pFRG/RTN neurons induced by hypercapnia. The discrepancy may be due to differences among recording sites and experimental conditions as well as the different ages of animals used.

Phox2b-positive cells in the RTN express NK1 receptors and substance P is thought to have a significant role in central chemoreception (Nattie & Li, 2006; Takakura *et al.* 2008). It has been suggested that substance P is released by mainly serotonergic neurons in the vicinity of the RTN neurons (Mulkey *et al.* 2007). In slice preparations from 7- to 10-day-old rats, substance P induced an increase in the discharge rate of RTN chemosensitive neurons in the presence of antagonists of glutamate, glycine, GABA and purinergic receptors, suggesting that a postsynaptic mechanism is primarily responsible for activation of RTN neurons by this neuropeptide (Mulkey *et al.* 2007). Indeed, similar to hypercapnic stimulation, substance P induced a depolarizing response in the pFRG/RTN neurons accompanied by an increase in input resistance (Fig. 4). However, the membrane depolarization induced by hypercapnia was still preserved after the depolarizing response by substance P was depressed. Thus, the NK1 receptor is not necessary for the CO_2 response of pFRG/RTN neurons.

The depolarization was accompanied by an increase in input resistance of parafacial neurons, consistent with an involvement of potassium channels in response to hypercapnia as suggested by previous studies (Kawai *et al.* 2006; Guyenet *et al.* 2008). However, it is unknown which type of potassium channels are involved in the hypercapnic-induced depolarization (Putnam *et al.*

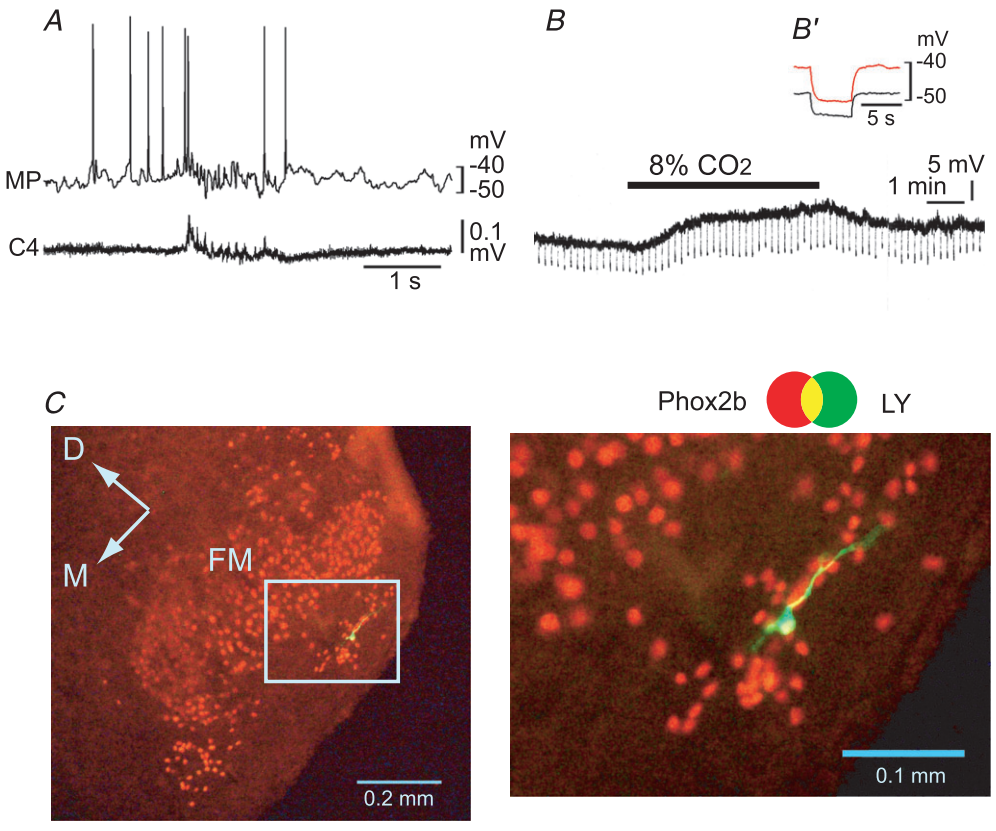

Figure 6. Effects of low Ca^{2+}–high Mg^{2+} + Cd^{2+} on the CO_2/H^+ response of a rostral pFRG/RTN neuron
A, burst pattern in the control solution. MP, membrane potential trace; C4, fourth cervical ventral root activity. *B*, membrane potential response to hypercapnic stimulation (2% CO_2 → 8% CO_2) in the presence of 0.5 μM TTX + 0.1 mM Cd^{2+} in low Ca^{2+}–high Mg^{2+} solution. Negative deflections of the baseline membrane potential are proportional to input resistance. *B′*, a faster sweep representation (average of 5 traces) of the membrane potential response to application of 20 pA hyperpolarizing square current pulses in 2% CO_2 (black trace) and 8% CO_2 (red trace). Note that application of 8% CO_2 induced membrane depolarization and an increase in input resistance. *C*, location of the recorded neuron stained by Lucifer yellow (LY, green). This neuron is Phox2b positive (red). Right panel, higher magnification of the highlighted square in the left image. FN, facial nucleus; D, dorsal; M, medial.

2004; Jiang *et al.* 2005; Guyenet *et al.* 2010*b*). In low Ca^{2+}–high Mg^{2+} ($+Cd^{2+}$) solution, membrane depolarization was not accompanied by an increase in the input resistance in half of the tested neurons despite the membrane depolarization. Kawai *et al.* (2006) reported that 20% of tested neurons showed membrane depolarization that was resistant to K^+ channel blockers and was not associated with an increase in the input resistance in response to hypercapnic stimulation (Kawai *et al.* 2006). Thus, it is possible that mechanisms other than ionic channels are involved in the hypercapnic-induced membrane depolarization in some neurons (Putnam, 2010). It is not clear whether the neurons that showed loss of the hypercapnia-induced conductance change in the present study were equivalent to examples of 20% neurons reported by Kawai (2006) or whether unknown effects were exerted on neurons by treatment with low Ca^{2+}–high Mg^{2+} ($+Cd^{2+}$). Although treatment with low Ca^{2+}–high Mg^{2+} may diminish an involvement of K^+ channels in membrane depolarization and unmask ionic channel-independent mechanisms, future studies are required to clarify the detailed mechanism.

In conclusion, hypercapnic stimulation depolarized the rostral pFRG/RTN neurons expressing Phox2b in neonatal rats, even after blockade of ATP or NK1 receptors as well as blockade of Ca^{2+} channels in the presence of TTX. Thus, this group of neurons was postsynaptically CO_2 sensitive without a contribution from calcium-dependent presynaptic or glial components. The CO_2 sensitivity is linked mainly to closure of the potassium channels of the postsynaptic membrane and it is important for future studies to clarify which type of potassium channels are involved in this response.

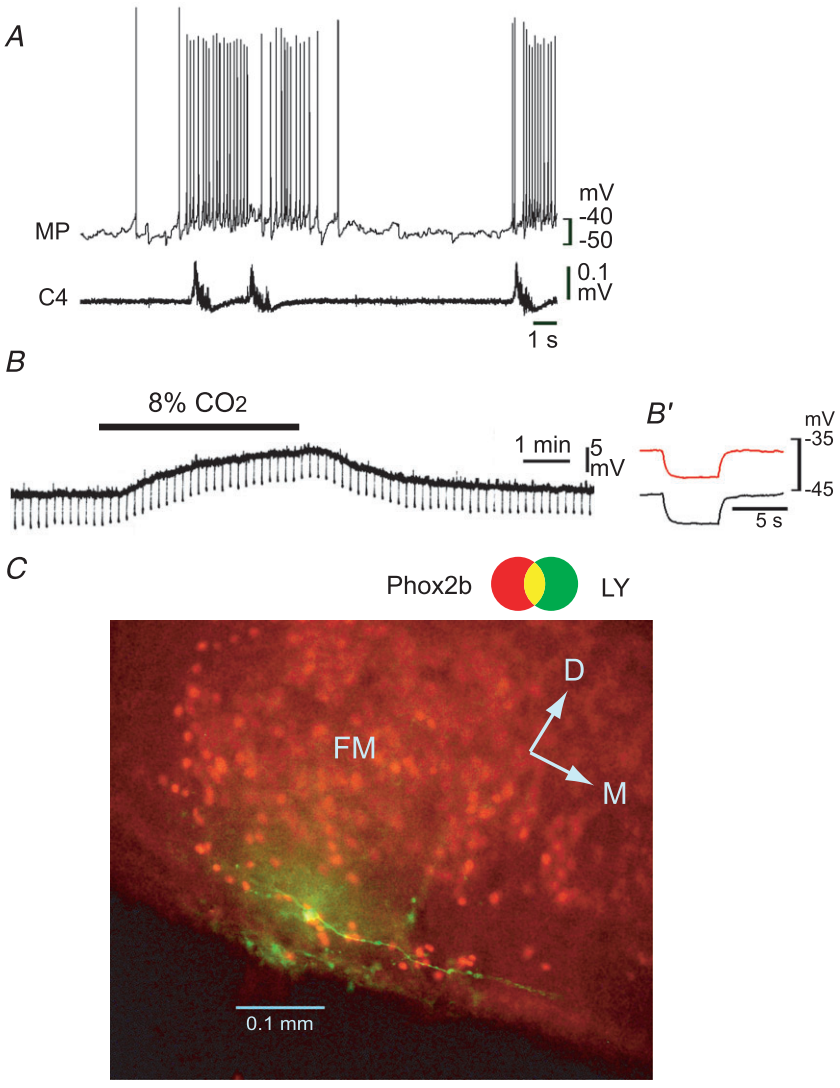

Figure 7. Effects of low Ca^{2+}–high Mg^{2+} + Cd^{2+} on the CO_2/H^+ response of a rostral pFRG/RTN neuron that did not show an increase in the input resistance
A, burst pattern in control solution. MP, membrane potential trace; C4, fourth cervical ventral root activity. *B*, membrane potential response to hypercapnic stimulation (2% CO_2 → 8% CO_2) in the presence of 0.5 μM TTX + 0.1 mM Cd^{2+} in low Ca^{2+}–high Mg^{2+} solution. Negative deflections of the baseline membrane potential are proportional to input resistance. *B′*, a faster sweep representation (average of 5 traces) of the membrane potential response to application of 20 pA hyperpolarizing square current pulses in 2% CO_2 (black trace) and 8% CO_2 (red trace). Note that application of 8% CO_2 induced membrane depolarization but the input resistance was not increased. *C*, location of the recorded neuron stained by Lucifer yellow (LY, green). This neuron is Phox2b positive (red). FN, facial nucleus; D, dorsal; M, medial.

References

Ballanyi K, Ruangkittisakul A & Onimaru H (2009). Opioids prolong and anoxia shortens delay between onset of preinspiratory (pFRG) and inspiratory (preBotC) network bursting in newborn rat brainstems. *Pflugers Arch* **458**, 571–587.

Drummond GB (2009). Reporting ethical matters in *The Journal of Physiology*: standards and advice. *J Physiol* **587**, 713–719.

Gourine AV, Kasymov V, Marina N, Tang F, Figueiredo MF, Lane S, Teschemacher AG, Spyer KM, Deisseroth K & Kasparov S (2010). Astrocytes control breathing through pH-dependent release of ATP. *Science* **329**, 571–575.

Guyenet PG, Stornetta RL, Abbott SB, Depuy SD, Fortuna MG & Kanbar R (2010*a*). Central CO_2 chemoreception and integrated neural mechanisms of cardiovascular and respiratory control. *J Appl Physiol* **108**, 995–1002.

Guyenet PG, Stornetta RL & Bayliss DA (2008). Retrotrapezoid nucleus and central chemoreception. *J Physiol* **586**, 2043–2048.

Guyenet PG, Stornetta RL & Bayliss DA (2010*b*). Central respiratory chemoreception. *J Comp Neurol* **518**, 3883–3906.

Jiang C, Rojas A, Wang R & Wang X (2005). CO_2 central chemosensitivity: why are there so many sensing molecules? *Respir Physiol Neurobiol* **145**, 115–126.

Kawai A, Onimaru H & Homma I (2006). Mechanisms of CO_2/H^+ chemoreception by respiratory rhythm generator neurons in the medulla from newborn rats *in vitro*. *J Physiol* **572**, 525–537.

Mulkey DK, Rosin DL, West G, Takakura AC, Moreira TS, Bayliss DA & Guyenet PG (2007). Serotonergic neurons activate chemosensitive retrotrapezoid nucleus neurons by a pH-independent mechanism. *J Neurosci* **27**, 14128–14138.

Mulkey DK, Stornetta RL, Weston MC, Simmons JR, Parker A, Bayliss DA & Guyenet PG (2004). Respiratory control by ventral surface chemoreceptor neurons in rats. *Nat Neurosci* **7**, 1360–1369.

Nattie E & Li A (2006). Neurokinin-1 receptor-expressing neurons in the ventral medulla are essential for normal central and peripheral chemoreception in the conscious rat. *J Appl Physiol* **101**, 1596–1606.

Onimaru H & Dutschmann M (2012). Calcium imaging of neuronal activity in the most rostral parafacial respiratory group of the newborn rat. *J Physiol Sci* **62**, 71–77.

Onimaru H & Homma I (1992). Whole cell recordings from respiratory neurons in the medulla of brainstem-spinal cord preparations isolated from newborn rats. *Pflugers Arch* **420**, 399–406.

Onimaru H & Homma I (2003). A novel functional neuron group for respiratory rhythm generation in the ventral medulla. *J Neurosci* **23**, 1478–1486.

Onimaru H, Ikeda K & Kawakami K (2008). CO_2-sensitive preinspiratory neurons of the parafacial respiratory group express Phox2b in the neonatal rat. *J Neurosci* **28**, 12845–12850.

Onimaru H, Ikeda K & Kawakami K (2009). Phox2b, RTN/pFRG neurons and respiratory rhythmogenesis. *Respir Physiol Neurobiol* **168**, 13–18.

Putnam RW (2010). CO_2 chemoreception in cardiorespiratory control. *J Appl Physiol* **108**, 1796–1802.

Putnam RW, Filosa JA & Ritucci NA (2004). Cellular mechanisms involved in CO_2 and acid signaling in chemosensitive neurons. *Am J Physiol Cell Physiol* **287**, C1493–C1526.

Ruangkittisakul A, Schwarzacher SW, Secchia L, Poon BY, Ma Y, Funk GD & Ballanyi K (2006). High sensitivity to neuromodulator-activated signaling pathways at physiological $[K^+]$ of confocally imaged respiratory center neurons in on-line-calibrated newborn rat brainstem slices. *J Neurosci* **26**, 11870–11880.

Stornetta RL, Moreira TS, Takakura AC, Kang BJ, Chang DA, West GH, Brunet JF, Mulkey DK, Bayliss DA & Guyenet PG (2006). Expression of Phox2b by brainstem neurons involved in chemosensory integration in the adult rat. *J Neurosci* **26**, 10305–10314.

Suzue T (1984). Respiratory rhythm generation in the *in vitro* brain stem–spinal cord preparation of the neonatal rat. *J Physiol* **354**, 173–183.

Takakura AC, Moreira TS, Stornetta RL, West GH, Gwilt JM & Guyenet PG (2008). Selective lesion of retrotrapezoid Phox2b-expressing neurons raises the apnoeic threshold in rats. *J Physiol* **586**, 2975–2991.

Wenker IC, Kreneisz O, Nishiyama A & Mulkey DK (2010). Astrocytes in the retrotrapezoid nucleus sense H^+ by inhibition of a Kir4.1–Kir5.1-like current and may contribute to chemoreception by a purinergic mechanism. *J Neurophysiol* **104**, 3042–3052.

Author contributions

H.O. designed and performed the *in vitro* electrophysiological recordings, immunohistochemistry, analysed the data and wrote the manuscript. K.I. and K.K. contributed to immunohistochemistry and edited the manuscript. All authors approved the final version.

Acknowledgements

This work was supported by Grants-in Aid for Scientific Research (KAKENHI: 19500277, 22500296).